Lithuanian Journal of Physics, Vol. **61**, No. 3, pp. 191–204 (2021)

EFFECT OF SPRING GRASS FIRES ON INDOOR AIR QUALITY IN AIR-CONDITIONED OFFICE BUILDING

J. Pauraitė [a], I. Garbarienė [a], A. Minderytė [a], V. Dudoitis [a], G. Mainelis [b], L. Davulienė [a], I. Uogintė [a], K. Plauškaitė [a], and S. Byčenkienė [a]

[a] *Department of Environmental Research, SRI Center for Physical Sciences and Technology, Savanorių 231, 02300 Vilnius, Lithuania*

[b] *Rutgers, The State University of New Jersey, 14 College Farm Road, New Brunswick, NJ 08901, United States*

Email: julija.pauraite@ftmc.lt

Received 20 January 2021; revised 15 April 2021, accepted 16 April 2021

Open biomass burning (OBB) is a significant air pollution source, but it is still not clear to what extent OBB events affect indoor air quality [1]. Outdoor and indoor measurements of submicron particulate matter (PM1) were conducted on 25–29 April (2019) in the capital city Vilnius (Lithuania). Fires from neighbouring countries (Belarus, Ukraine and Russia) and in the vicinity of Vilnius broke out during the measurement campaign. The temporal evolution and transport of OBB plume were investigated by combining the air mass backward trajectory analysis and fire satellite observation (MODIS) database. Measurements of the PM1 chemical composition in real-time were performed using an aerosol chemical speciation monitor (ACSM) and an aethalometer. Organic matter was the clearly dominant component, accounting for >70%, in both indoor and outdoor PM1. The air filtering system of the office building removed approximately up to 55% of PM1. Despite a significantly lower PM1 pollution level in the office, highly acidic indoor PM1 could have harmful effects on the human health. Source apportionment of particulate carbonaceous matter revealed a significant importance of OBB-related particles (average 56%) to indoor air.

Keywords: organic aerosol, black carbon, indoor air quality, biomass burning

PACS: 92.60.Sz, 92.60.Mt, 92.60.hf

1. Introduction

Spring grass fires (or open biomass burning – OBB) is a significant air pollution source, with adverse impacts on global, regional and local air quality, public health and climate [2–5]. OBB occurs globally with highly variable biomass types (wood, shrub, grass, vegetation and crop residues) and burning conditions [6]. OBB generally emits a high amount of gaseous compounds (CO_2, CO, NO_x, volatile organic compounds – VOCs) and carbonaceous aerosols (e.g. equivalent black carbon (eBC) and organic carbon (OC)) to the atmosphere in a short period of time [7, 8]. However, it was estimated that OBB globally contributed to ~40% of the annual average submicron eBC emission and ~65% of primary OC emission [3]. Quantitative assessment of the contribution of biomass burning to carbonaceous aerosol has focused on the molecular markers, such as levoglucosan, approach [9, 10]. Recently, the characterization of chemical composition and potential sources of submicron aerosol particles (PM_1) has improved with the advent of aerosol mass spectrometric technique (AMS, aerosol chemical speciation monitor – ACSM). Previous studies demonstrated that the application of factor analysis approach on ACSM derived mass spectra of organic species permits the identification of various organic aerosol (OA) sources and photochemical ageing processes [11, 12]. The source apportionment model based on light absorption properties of carbonaceous materials (aethalometer model) has been widely used to separate combustion (fossil fuel and biomass burning) and non-combustion sources (secondary organic aerosol) of carbonaceous aerosol [13, 14].

Lithuania and surrounding countries are frequently affected by high-pollution events in early

spring due to illegal grass burning for land clearing [15, 16]. Long-term measurements of carbonaceous aerosols revealed the yearly occurrence of intense biomass/grass burning events during March–April related to the regional aerosol transport from the Kaliningrad region, Ukraine and the south-western part of Russia surrounding the Black Sea [15–18]. Moreover, forest and grassland burning phenomena could significantly influence indoor pollution levels [19].

The quality of indoor air has become a global concern during last decades as people spend most part of the day inside of buildings [20, 21]. Studies indicate that the indoor air quality is influenced by the outdoor air quality mainly due to the building ventilation factor [21, 23]. Modern energy-conserving buildings have improved energy conservation through reducing exchanges between outdoor and indoor air, and synthetic materials and chemical products have been extensively used in these airtight buildings. Therefore, the selection of ventilation regimes and monitoring of indoor sources become important [24, 25]. Numerous studies focused on indoor air quality within residential buildings [23, 26–28]. However, the impact of short-term air pollution events caused by open biomass/grass burning on the office building micro-environment has not been extensively investigated.

The aim of this study was to evaluate the influence of local/regional open biomass burning events on indoor air quality and sources distribution in a mechanically ventilated office building.

2. Materials and methods

2.1. Measurement site

Complex measurements were performed on 25–26 April in indoor air and on 26–29 April 2019 in outdoor air. The sampling site was ~370 km northwest from active fire regions. The investigation was carried out at a newly built (2015) low-energy (B class) building of the Center for Physical Sciences and Technology in Vilnius, Lithuania (54°43′24″N, 25°19′36″E). The instruments were placed in the vacant meeting room on the 2nd floor. The door of the meeting room was kept closed to avoid air exchange with other rooms and minimize the impact of indoor PM_1 sources. During the outdoor measurement period inlets were positioned outside. The mechanical/forced air ventilation system in this room is equipped with G4/F7 filters. The pre-filter G4 removes particles in the >10 μm size range. The F7 filter removes particles within 0.3–10 μm. The rate of air flow into and out of the meeting room was 320 and 120–320 $m^3 h^{-1}$ (depending on CO_2 amount), respectively. The sampling site is located 6–7 km northeast from the centre of Vilnius. The local traffic is usually an important source of PM_1 in Vilnius (25%) [29]. Because of the heating season termination 10 days earlier, during this period the influence of domestic heating was negligible. The biomass burning (BB) source could be related to OBB (e.g. grassland burning, forest and garden waste burning) that routinely shows a significant contribution during spring in Lithuania.

2.2. Instrumentation

Equivalent black carbon (eBC) measurements were performed using an aethalometer (Model AE31 Spectrum, manufactured by *Optotek*, Slovenia). The optical transmission of carbonaceous aerosol particles was measured sequentially at seven wavelengths λ (0.37, 0.45, 0.52, 0.59, 0.66, 0.88 and 0.95 μm) with 2 min intervals and 3.9 l/min flow rate. The aethalometer model [13] was applied in order to attribute eBC mass concentration to biomass burning and fossil fuel combustion (eBC_{BB} and eBC_{FF}, respectively). Filter-based optical measurements contain systematic errors due to filter loading, 'shadowing', multiple scattering and other effects [30]. Thus, the correction suggested by Weingartner was applied in this study; this method is described in more detail in the original article by the author [31].

During this study, the concentration of organic aerosol (OA) together with secondary inorganic aerosol (SIA) was measured by an aerosol chemical speciation monitor ACSM (*Aerodyne Research, Inc.*, Billerica, MA, USA) which operated with a time resolution of ~30 min. A detailed description of the ACSM operation and data analysis are given in Ref. [17], Ulevicius et al. (2016).

2.3. Models and additional tools

Due to short both indoor and outdoor measurement campaigns, positive matrix factorization

analysis could not be statistically robust. Therefore, an alternative source apportionment was implemented. The analysis consisted of the assessment of different carbonaceous species (CM) and OA mass spectra attribution for each of them.

The aethalometer model was originally developed in order to quantify eBC sources (fossil fuel and biomass burning). However, a few studies adapted an aethalometer model to quantitatively estimate the contribution of particulate carbonaceous matter (eBC and organic mass (OM)) from fossil fuel and biomass burning emissions, using the different light absorption parameters of these sources [32–35]. We applied this approach to apportion the total carbonaceous material (CM) mass concentration to biomass burning (CM_{BB}), fossil fuel (CM_{FF}) and non-absorbing material (CM_{NA}) according to the following equations:

$$CM = OM + eBC, \quad (1)$$

$$CM = CM_{FF} + CM_{BB} + CM_{NA}, \quad (2)$$

$$CM = c_1 \cdot b_{absFF}(950\,nm) + c_2 \cdot b_{absBB}(470\,nm) + c_3. \quad (3)$$

In our study, the total CM is the sum of eBC, measured by the aethalometer, and OM measured by ACSM. The CM mass concentration was regressed against b_{absFF} (950 nm) and b_{absBB} (470 nm) for the estimation of contribution of transport emissions (CM_{FF}) and biomass burning (CM_{BB}) sources. The coefficients c_1 and c_2, calculated by Eq. 3, are related to the light absorbing CM mass of both sources. The intercept c_3 reflects the contribution of non-absorbing carbonaceous materials (CM_{NA}).

In our study, the mass spectra of different CM species were estimated by attributing the time series of OA to the related *m/z* signals profiles. Based on bilinear modelling [11], OA can be presented as the product of two matrices. The first one comprises the time series of mass concentration (TS) while the second one is the mass spectrum (MS) or source profiles of individual OA factors

$$(OA) = (TS) \times (MS) + (E), \quad (4)$$

where (E) is the matrix of residuals. In our study, the time series of CM_{BB}, CM_{FF} and CM_{NA} were used as individual TS [11]:

$$OA_{ij} = \sum_{p=1}^{p} TS_{ip} MS_{pj} + E_{ij}, \quad (5)$$

Here *j* refers to an ion fragment at time step *i* for a given factor *p*. As a result, individual MS of OA for each CM species were obtained. The ME-2 engine tool [36] was used for the calculation.

The mass spectra of outdoor and indoor identified factors have been compared using the θ angle analysis introduced by Kostenidou et al. (2009) [37]. The θ angle is a measure of similarity between two mass spectra ($\theta < 15°$ high similarity; $15° < \theta < 30°$ partial similarity; $\theta > 30°$ different spectra).

Wildfire events were explored using the fire information for the resource management system (FIRMS) which distributes satellite observation from the NASA's moderate resolution imageing spectroradiometer (MODIS) and the visible infrared imaging radiometer suite (VIIRS).

Air mass backward trajectories were calculated using the hybrid single-particle Lagrangian integrated trajectory (HYSPLIT4) [38] model with the global data assimilation system (GDAS) meteorological databases at the NOAA Air Resources Laboratory's web server (NOAA HYSPLIT Trajectory Model. Ready.Noaa.Gov, 2020, https://www.ready.noaa.gov/hypub- bin/trajtype.pl?runtype=archive). To provide a better view of which air masses had influenced the rise of aerosol concentrations, trajectory frequencies were calculated using the NOAA HYSPLIT model, where the 72 h backward trajectory frequency was calculated from a single location (sampling site) at 500 m height every 6 h. The sum of frequency of trajectories passed over a grid cell (1.0° × 1.0°) was normalized by the total number of trajectories [39].

In our study, aerosol pH was evaluated by a thermodynamic equilibrium model ISORROPIA-II [40]. This method calculates the equilibrium partitioning the given total concentration of different species. ISORROPIA-II determines the system of equilibrium equations and solves them for the equilibrium state using the chemical potential method [40]. pH was evaluated using aerosol secondary inorganic chemical components (NH_4^+, NO_3^-, SO_4^{2-}, Cl^-) measured by ACSM together with temperature (*T*) and relative humidity (RH).

RH, *T* and time series of NO_2 were measured at the nearby (2 km away) located monitoring station.

2.4. Meteorological condition during the study period

The average daytime temperature on 25–29 April was about +22°C (positive 1.2–2.9° anomaly). The highest daytime temperature was fixed at +29°C. The average night-time temperature was +10–12°C. The direction of the wind was mainly from east during the whole study period. The wind speed was relatively low and varied between 1 and 7 m s^{-1}. The air pressure ranged from 1040 to 1200 hPa. 2019 April was one of the driest months in the last decade. During the day, most of the time slightly or moderately unstable conditions with a boundary layer depth up to 1.5–2.0 km were dominant. On 25–29 April, in most of Lithuania there was no precipitation at all or the amount of precipitation did not reach 5.0 mm (0.0–0.1 standard precipitation rate – SPR). Due to the abovementioned meteorological conditions, the high fire risk (Level 4) was registered in all Lithuanian municipalities. On 25–29 April 2019, there were 266 (about 125 ha burnt area) fires in the open territory (forest, grass, etc.) in Lithuania. 100 of them (about 52.5 ha) were in the Vilnius District (http://pagd.lrv.lt/lt/paros-ivykiai/2019-m-1/2019-m-balandis, last visited on 13 April 2021). The following indoor meteorological conditions were fixed: RH = 40% and T = 21°C.

2.5. Fire event

The active fire map created using the FIRMS MODIS database confirms the great abundance of active fire events in the regional area eastwards from Vilnius for the period of 25–29 April (Fig. 1(a)). The highest density of the active fire locations was present in the Kaliningrad Region of Russia that is 300–400 km to east from the measurement station. Meanwhile, another OBB located near the border of Belarus and Ukraine was ~370 km southeast from Vilnius.

Figure 1(b) shows the smoke surface concentration measured on 25 April. It is worth noting that the smoke concentration was enhanced due to large quantities of active fires as the highest concentrations are observed over the regions with denser locations of active fires. Furthermore, Fig. 1(c) presents a backward 72 h trajectory frequency plot where the arrival of air parcels originating aloft over wildfire regions and other regions with a high number of active fire locations is apparent. Thus, the influence of smoke transport for surface-level air quality in Vilnius is evident. On 25 April, air parcels crossed the central part of Ukraine and then southwest of Belarus which demonstrates that the air parcels passed over the OBB region and other active fire locations and later descended to the surface level in the area of Vilnius where enhanced PM levels were recorded. The backward trajectories of air parcels arriving to Vilnius show a very similar path on 25–27 April where the air masses originate aloft presence of wildfires. The mass concentration of particulate matter with a diameter up to 10 μm (PM_{10}) in the capital city Vilnius (Lithuania) rose up to 90 $\mu g\ m^{-3}$ on 25–27 April. The daily PM_{10} concentration exceeded the European Union's

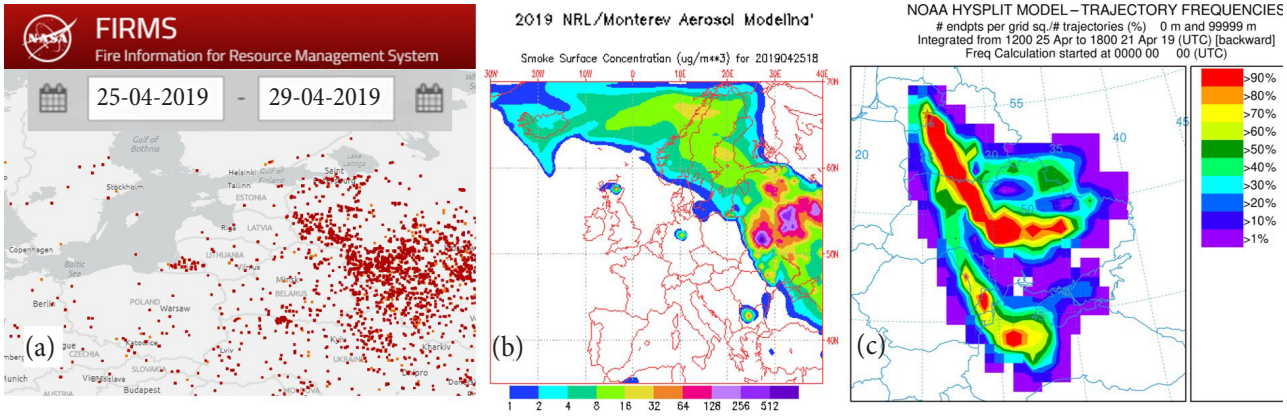

Fig. 1. Locations of active fire detections from the FIRMS MODIS database for the time period from 25 to 29 April (a), NRL model results showing smoke surface concentrations for 25 April (b), NOAA HYSPLIT model backward 72 h trajectory frequency plot from a starting location at the measurement station in Vilnius at 500 m AGL (c).

established limit value (50 μg m^{-3}) up to 1.6 times (http://oras.gamta.lt/files/Oras_190426v.pdf, last visited on 13 April 2021). Later on 28–29 April, the air mass transport from northeast prevailed. During the following period, the density of active fire was significantly lower, resulting in the decrease of PM_{10} concentration (average 30 μg m^{-3}). However, this PM_{10} level exceeded the typical non-episodic condition in Vilnius (16.8±8.4 μg m^{-3}) (average ± standard deviation). Consequently, it can be concluded that air parcels from the southeast region had a significant influence on enhanced pollutant concentrations in Vilnius on 25–29 April.

We used the records of cloud-aerosol lidar and infrared pathfinder satellite observations (CALIPSO) to investigate the sources of aerosol particles and the vertical distribution of the 25 April 2019 pollution episode in Vilnius. The satellite observation from CALIPSO showed (Fig. 2) that aerosol load below 3 km was classified as polluted dust, smoke and polluted continental. These findings indicated that the regional/local biomass burning events were most likely the cause of enhanced pollution levels in Vilnius, Lithuania.

3. Results

3.1. PM_1 variation, chemical composition and acidity

The time series of PM_{10} and PM_1 chemical composition (organic compounds, sulphate, nitrate, ammonium and black carbon) and their relative contributions are presented in Fig. 3. The average mass concentration of PM_1 of outdoor measurements was 43.2±22.3 μg m^{-3} while the average PM_1 concentration of indoor air reached 8.8±2.7 μg m^{-3}. The concentration of PM_1 (in both outdoor and indoor measurements) was strongly correlating with PM_{10} (measured only outdoors), $r = 0.7$, indicating a substantial contribution of outdoor sources to PM_1 levels in office buildings. In order to evaluate the indoor air filtering, the PM_1 dataset was compared to the outdoor PM_{10} measurements. For the outdoor dataset, PM_1 showed a significant contribution to PM_{10} (58±23%) while the indoor PM_1 was 26±6% of the outdoor PM_{10}. Thus, the air filtering system of the building removed approximately up to 55% of PM_1.

The outdoor PM_1 mass concentration was dominated by organic compounds (37.9±19.2 μg m^{-3}), followed by SO_4^{2-} (2.2±0.5 μgm^{-3}), NO_3^- (2.1±1.3 μg m^{-3}), eBC (0.9±0.6 μg m^{-3}) and NH_4^+ (0.8±0.3 μg m^{-3}) (Fig. 3(a)). During the intense OBB event (25–26 April), a significant enhancement of organic compounds (up to 67.7 μg m^{-3}), NO_3 (4.1 μg m^{-3}) and eBC (3.1 μg m^{-3}) mass concentration was registered. The average mass contribution of PM_1 species during the OBB event was organic aerosol (87%), NO_3^- (5%), SO_4^{2-} (5%), NH_4^+ (2%) and eBC (2%) (Fig. 3(b)).

The average mass concentrations of PM_1 chemical components in office air were significantly lower (7.0±2.2 μg m^{-3} for organics, 1.1±0.3 μg m^{-3} for sulphate, 0.3±0.2 μg m^{-3} nitrate, 0.3±0.1 μg m^{-3} ammonium and 0.2±0.1 μg m^{-3} eBC). However, the chemical

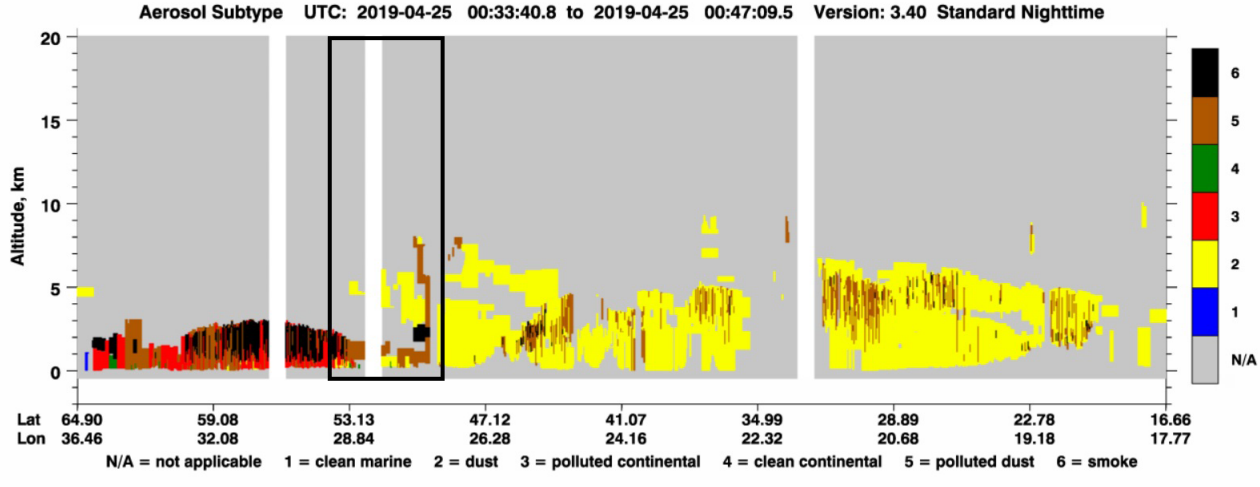

Fig. 2. CALIPSO-derived vertical profile of aerosol subtypes over Vilnius on 25 April 2019.

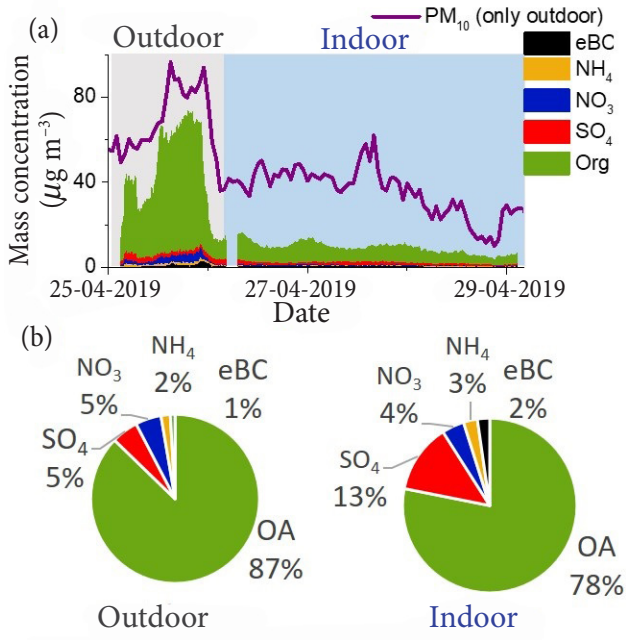

Fig. 3. Time series of PM_1 species (a) and their contributions to total PM_1 (b) for outdoor and indoor measurements. Time series of PM_{10} (a) was measured only outdoor.

composition of PM_1 was similar in both outdoor and indoor environments (Fig. 3). The highest difference in the PM_1 composition between outdoor and indoor measurements was observed for SO_4^{2-} contribution (5 and 13%, respectively).

Such enhancement in the contribution of sulphate in the office building resulted in changes of PM_1 acidity. As seen in Fig. 4, the average aerosol pH of indoor aerosol was significantly lower than the outdoor one. In our study, in both outdoor and indoor environments, aerosol pH negatively correlated with SO_4^{2-} (r = –0.63 and r = –0.62, respectively). This is in agreement with previous studies [41, 42], which have shown that under low aerosol liquid water content conditions the increase in SO_4^{2-} levels was followed by decreased aerosol pH. Furthermore, the same studies showed that SO_4^{2-} had a greater effect on aerosol pH than NO_3^-. Meantime in our study, only in the outdoor measurements a possible link between aerosol pH and NO_3^- was observed (r = 0.82) while no such correlation was observed in the indoor measurements. A similar pattern was observed between the aerosol pH and NH_4^+ concentration. Chen et al. (2019) [41] concluded that increased NH_4^+ resulted in a slight increase of aerosol pH. In agreement with the latter, in our study of outdoor measurements, the closest to neutral aerosol pH (pH 4.0–4.8) was observed with the highest NH_4^+ concentrations. The same link was not observed for the indoor dataset (Fig. 4(b)).

Differences between indoor and outdoor aerosol pH could be caused by several factors. First of all, while outside the building the T and RH were on the average 16.8±4.2°C and 44±9%, respectively, the indoor air conditions were set to be constant with higher T (21°C) and significantly lower RH (25%). Ding et al. (2019) [42] showed that there was a significant decrease in pH with increased T, while

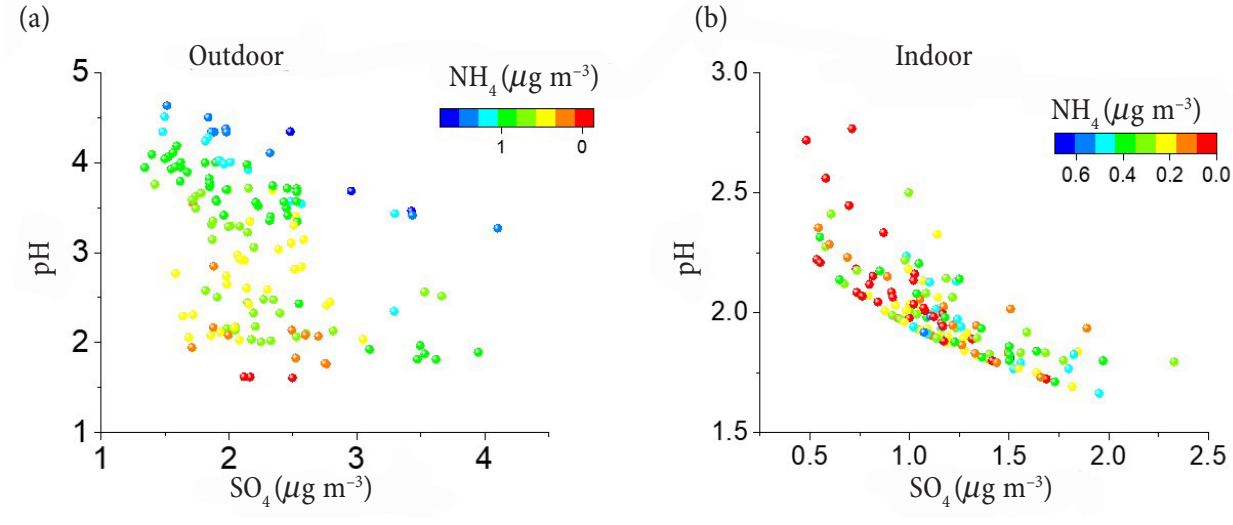

Fig. 4. Aerosol pH versus SO_4^{2-} mass concentration for outdoor (a) and indoor (b) measurements. Colour (online) plotting by NH_4^+ mass concentration.

the effect due to RH varied over different seasons. Meantime, the modelling results [41] revealed that warmer and dryer atmosphere led to lower aerosol pH because partitioning of ammonia to the condensed phase is less favoured. In addition, other parameters such as size distribution and aerosol liquid water content could play a significant role in aerosol pH alterations [42]. Guo et al. (2015) [43] underlined that low pH could affect the solubility of metals such as Fe and Cu which might increase the toxicity of redox metals. Furthermore, a recent study [41] underlined that pH ranging from 0 to 3 could be called 'sensitive window' where nitrate related gas-to-particle partitioning is sensitive to pH alterations. Thus, low levels of indoor aerosol pH could cause differences in particle formation processes and cause alterations in other parameters, such as toxicity. Despite the significantly lower PM_1 and concentrations of its chemical components in the office, highly acidic indoor PM_1 could have harmful effects on the human health. Therefore, additional study of various parameters of indoor air is needed.

3.2. Ageing properties of organic aerosol

Organic compounds were the most important constituents of PM_1, with a fraction of ~80% during the investigated period. The triangle plot [12] was used as a tool to explore possible sources and to assess OA atmospheric ageing properties. The triangle plot consists of f_{43} (intensity of *m/z* 43 normalized to OA) and f_{44} (intensity of *m/z* 44 normalized to OA) space with additional lines for the visualization (Fig. 5). Since photochemical ageing leads to the increase in *m/z* 44 fraction, the f_{44} axis can be considered as a proxy of ageing parameterization. Several studies showed that different positions in the triangle can be connected to specific OA sources [12, 44, 45]. The triangle space with f_{43} vs f_{44} range 0.03–0.07 and 0.10–0.14, respectively, could be related to long-range transport (LRT) biomass burning OA [45]. The area with the same f_{43} range but lower f_{44} values was assigned to local and fresh biomass burning OA while the area with higher f_{44} was linked to aged low-volatile OA [45]. In our study, most of outdoor data points were located at the area assigned to LRT biomass burning OA proving the previous hypothesis of a strong influence of OBB events. Several points were lower indicating the fresh biomass burning related emissions. 92% of the outdoor data points had f_{60} (intensity of *m/z* 60 normalized to OA) above the background level (no significant presence of the main signal of biomass burning tracer levoglucosan) of 0.003 [46], indicating that a great part of OA in Vilnius can be related to OBB emissions (OA-OBB). The average outdoor f_{60} values of OA-OBB were 0.005±0.001, additionally supporting that OA related to biomass burning from distance sources (LRT OA-OBB) exceeded those of local (fresh) biomass burning emissions.

Particles with even more advanced ageing processes were observed in the indoor measurements (f_{44} up to 0.25) (Fig. 5). Only 26% of indoor OA had f_{60} above 0.003 and could be attributed to biomass burning related OA (OA-BB). The mean indoor f_{60} values (0.002±0.001) of OA-BB were close to

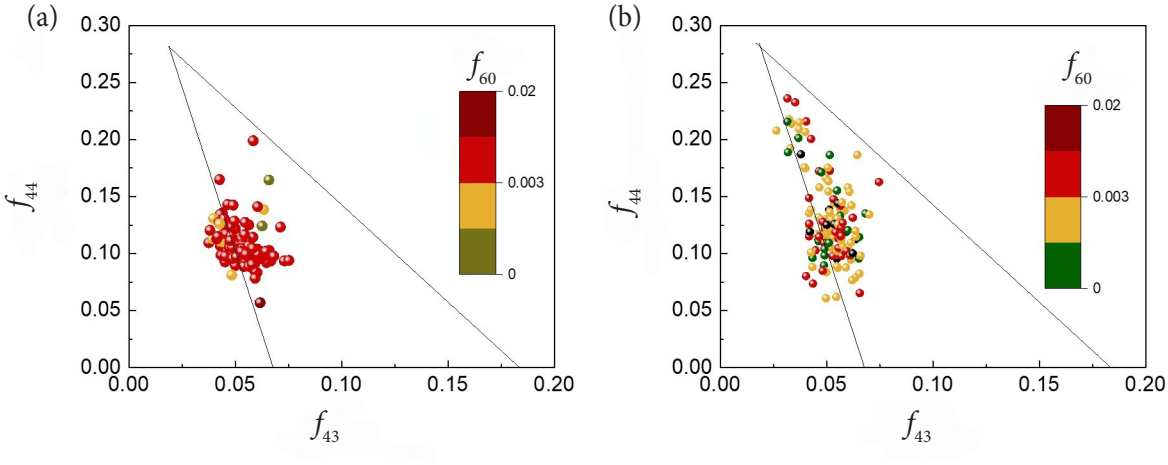

Fig. 5. Triangle plot of f_{43} versus f_{44} coloured (online) by f_{60} for outdoor (a) and indoor (b) measurements.

the background level. These could be explained by the dilution effect when the OBB plume is mixed with air masses containing organic aerosol particles of other origin. On the other hand, the gradual decay of f_{60} could return f_{60} to background values [47]. Recent studies highlighted that aged OA-BB had a weak signal of m/z 60, suggesting that f_{60} is not an effective tracer of aged OA-BB [44, 48].

3.3. Apportionment of carbonaceous aerosol sources

The apportionment of eBC sources based on the aethalometer model showed that the eBC_{BB} contribution to the eBC mass concentration was dominant for both outdoor and indoor measurements (68 and 67%, respectively) (Fig. 6). eBC_{FF} made up only 32–33% of eBC mass during the investigated period. The time series of eBC_{BB} correlated best with f_{60} ($r = 0.66$). Furthermore, the intensity of signal f_{60} was higher than 0.003. Therefore, increased outdoor levels of eBC_{BB} were associated with OBB events. Meanwhile, eBC_{FF} showed a moderate correlation with NO_2 in the gas phase ($r = 0.54$) strengthening the hypothesis of possible origin from fossil fuel combustion. In addition, the diurnal plot showed that the highest values of eBC_{FF} were reached during morning rush hours (from 7 to 10 am). Thus, these observations allowed to link eBC_{FF} to the traffic related emissions (Fig. 6). The previous study of eBC in Vilnius during the warm season under normal conditions showed a dominant influence of eBC_{FF} (92%) [49]. That finding suggested that the PM_1 chemical composition on 25–29 May 2019 was clearly unusual for Vilnius and was related with the OBB event. In our study, the contribution of eBC_{FF} and eBC_{BB} to the total eBC mass concentration remained unchanged in outdoor and indoor environments. Thus, both eBC_{FF} and eBC_{BB} were filtered in the indoor air with the same efficiency and therefore a high influence of OBB related eBC_{BB} remained significant.

In the case of CM, biomass burning (CM_{BB}) and non-absorbing carbonaceous materials (CM_{NA}) were found to account, respectively, for 87 and 13% of the total CM during the outdoor measurements. The average relative contribution

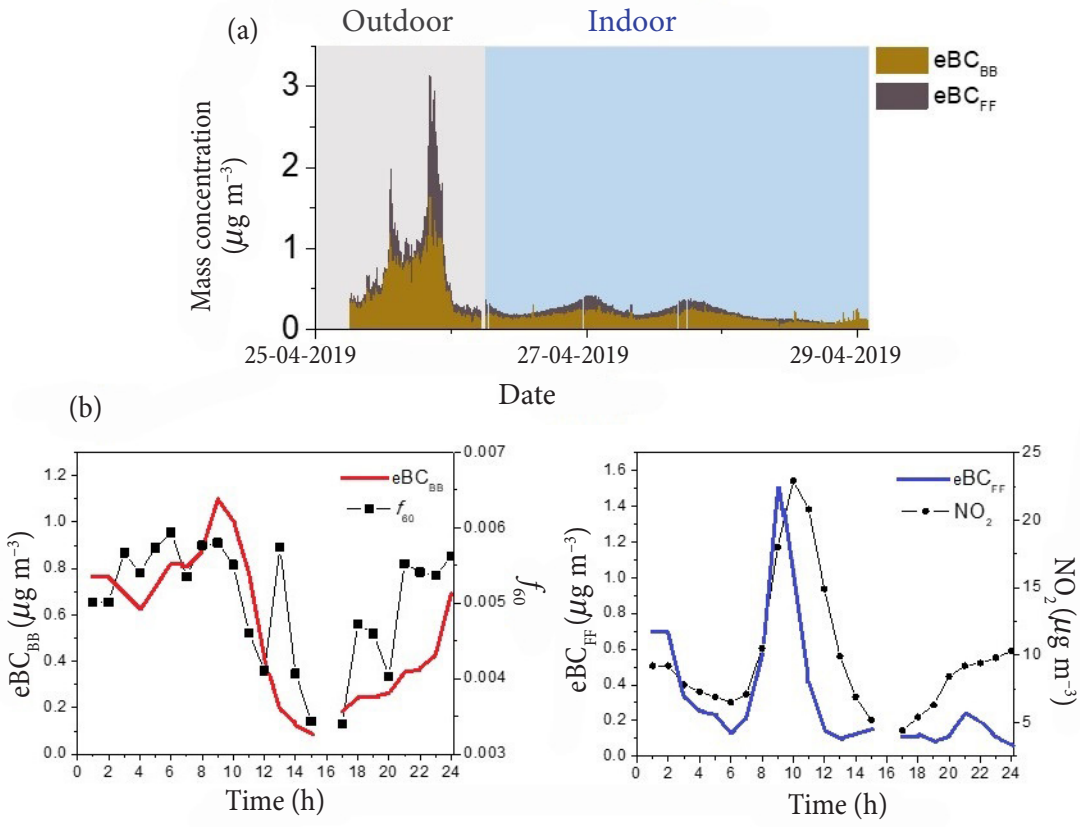

Fig. 6. Time series of the eBC_{BB} and eBC_{FF} mass concentrations (a) and the diurnal cycles (b) of eBC_{BB}, eBC_{FF}, f_{60} and NO_2 during the OBB event.

of indoor CM_{BB}, CM_{FF} and CM_{NA} was 56, 6 and 38%, respectively. The results of the model revealed a significant contribution of absorbing organic matter or brown carbon (BrC) to the CM mass concentration.

During the measurement campaign CM_{FF} contribution to the total CM was the lowest (0% in outdoor and 6% (0.47±0.29 $\mu g\ m^{-3}$) in indoor air). Due to low concentrations of CM_{FF} and no meaningful or robust aerosol mass spectra were attributed to this aerosol. The time series of CM_{BB} correlated well with eBC_{BB} ($r = 0.85$) and f_{60} ($r = 0.71$), suggesting that the CM source apportionment method is valid for our study and is an appropriate method for characterizing BB emissions. Furthermore, the CM_{BB} mass spectrum showed characteristics of both OA-BB (m/z 60) and oxygenated OA (m/z 18 and 44) (Fig. 7). This factor represents aged OA-BB or a mixture of primary OA-BB and secondary OA from other sources. It is possible that the traffic derived secondary OA can partially contribute to CM_{BB}.

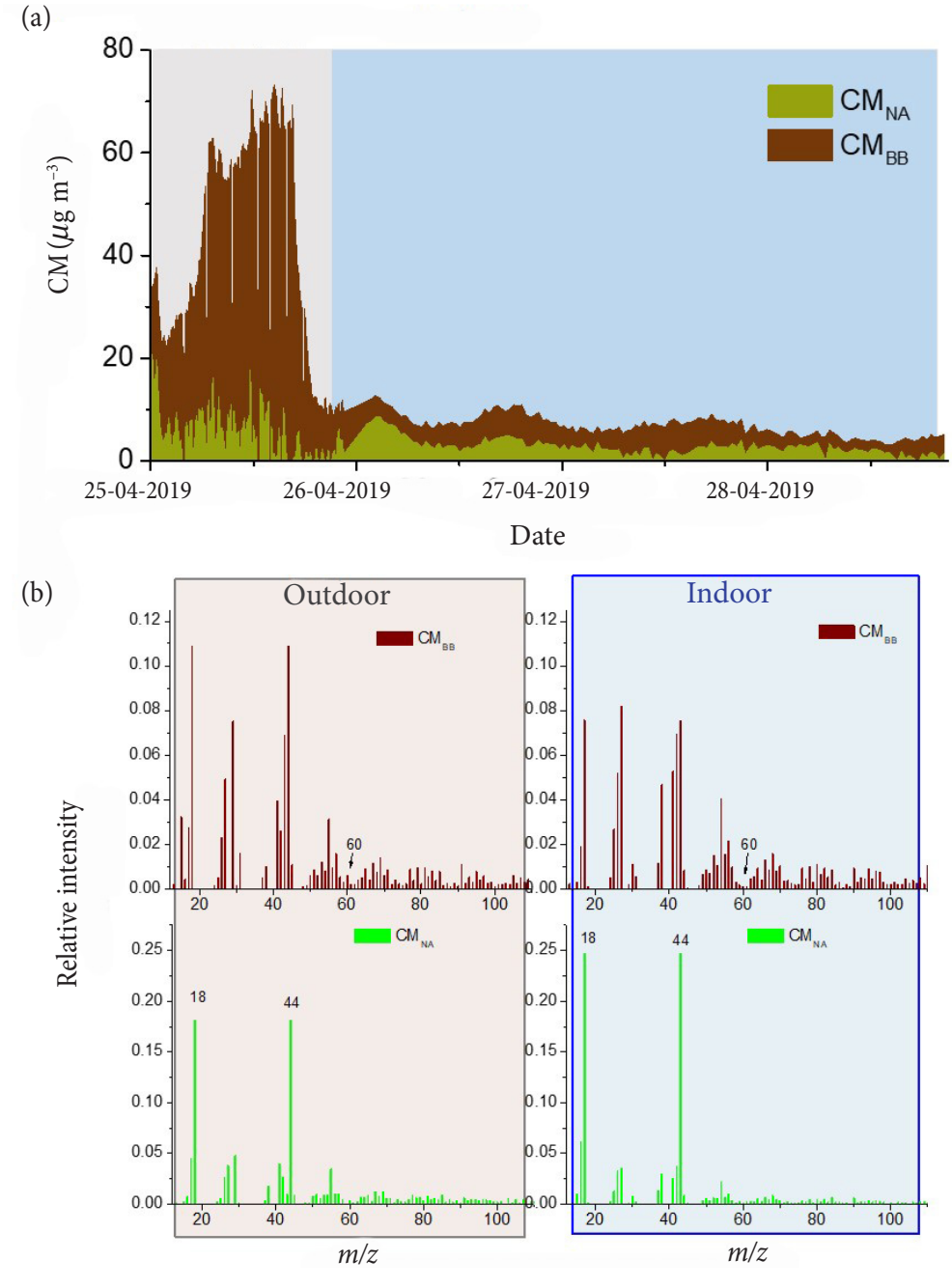

Fig. 7. Time series of each CM component obtained using an advanced aethalometer model (a) and its mass spectra for outdoor and indoor measurements (b).

However, the indoor data showed a negligible signal of f_{60} in the CM_{BB} profile (0.002±0.001) (Fig. 7). Moreover, a poor correlation between f_{60} and CM_{BB} was observed in the indoor samples, likely due to the photochemical degradation of levoglucosan [50]. Recent studies [44, 49] demonstrate that the mass spectral fingerprint of levoglucosan (f_{60}) cannot be used as BB tracer in aged BB emissions (>1 day). These findings suggest that the method of CM source apportionment based on optical properties is indeed a good BB indicator. Hence, the advanced aethalometer model was useful for the CM source apportionment of aged BB aerosol.

The CM_{NA} component, represented by the highest contribution of f_{44} (18 and 25% in outdoor and indoor air, respectively), was attributed to the processed OA. This is associated with the chemical ageing of OA during long-range transported OA.

The theta angle analysis showed that outdoor and indoor CM_{BB} mass spectra were slightly different ($\theta = 16°$). This is consistent with the chemical ageing of OA-OBB indoors. The CM_{NA} mass spectra in outdoor and indoor air were quite similar ($\theta = 11°$). Many similarities of the outdoor and indoor spectra of both CM_{BB} and CM_{NA} profiles indicated that carbonaceous particles originating outdoors were an important contributor to the indoor CM mass concentration.

These results demonstrate that even if the indoor air had lower CM levels, the influence of outdoor air was evident and therefore a significant importance of OBB related particles to indoor air was observed.

4. Conclusions

During the measurement campaign (25–29 April 2019), open biomass burning OBB occurred in the vicinity of Vilnius (Lithuania) and surrounding areas. The analysis of air mass backward trajectories and the results of satellite fire observation showed that the elevated concentration of PM_1 in Vilnius was related to large quantities of active fires in Belarus and Ukraine. During the whole measurement campaign, PM_1 mass concentration was dominated by organic aerosol OA in both outdoor and indoor environments the mass concentration of which on the average decreased from 37.9 to 7.0 $\mu g\ m^{-3}$, respectively.

The pH of PM_1 ranged between 2–4 and 1.7–2.5 outdoor and indoor, respectively. Lower pH was detected in PM_1 with a higher load of SO_4^{2-}. The aerosol pH analysis showed that due to specific meteorological conditions (low RH, 25%, and high T, 21°C) of the office air, pH levels were significantly lower and therefore could have led to changes in several PM processes and properties, including particle composition, reactivity, gas-particle partitioning and toxicity. Our observations revealed that the air filtering system of the building removed approximately up to 55% of PM_1.

The variation of f_{44}, f_{43} and f_{60} parameters allows us to discriminate BB from other sources and examine the evolution of biomass burning organic aerosol OA-BB. At the beginning of the OBB episode, long-range transported BB emissions contributed significantly to OA. On 27–29 April, organic aerosol was characterized by high f_{44} and low f_{60} values, due to the oxidation processes and ageing of BB plume. Due to the OBB event, biomass burning derived carbonaceous aerosol was dominant for both outdoor (eBC_{BB} = 68%, CM_{BB} = 87%) and indoor (eBC_{BB} = 67%, CM_{BB} = 56%) measurements. It can be concluded that the OBB event had a strong influence on the indoor air quality. Yet, additional studies of simultaneous indoor and outdoor air quality over OBB events are required before firm conclusions could be drawn.

Acknowledgements

This research was funded by Grant No. S-MIP-20-28 'Contribution of Outdoor Air Pollution to Indoor Air Quality and Inhaled Deposited Dose' from the Research Council of Lithuania. The authors also want to express their appreciation to the Environmental Protection Agency of Lithuania.

References

[1] P. Rajagopalan and N. Goodman, Improving the indoor air quality of residential buildings during bushfire smoke events, Climate **9**, 32 (2021), https://doi.org/10.3390/cli9020032

[2] A. Kocbach Bølling, J. Pagels, K.E. Yttri, L. Barregard, G. Sallsten, P.E. Schwarze, and C. Boman, Health effects of residential wood smoke particles: the importance of combustion conditions

and physicochemical particle properties, Part. Fibre Toxicol. **6**(1), 29 (2009), https://doi.org/10.1186/1743-8977-6-29

[3] T.C. Bond, S.J. Doherty, D.W. Fahey, P.M. Forster, T. Berntsen, B.J. DeAngelo, M.G. Flanner, S. Ghan, B. Kärcher, D. Koch, et al., Bounding the role of black carbon in the climate system: A scientific assessment, J. Geophys. Res. Atmos. **118**(11), 5380–5552 (2013), https://doi.org/10.1002/jgrd.50171

[4] Ö. Gustafsson, M. Kruså, Z. Zencak, R.J. Sheesley, L. Granat, E. Engström, P.S. Praveen, P.S.P. Rao, C. Leck, and H. Rodhe, Brown clouds over South Asia: biomass or fossil fuel combustion? Science **323**(5913), 495 (2009), https://doi.org/10.1126/science.1164857

[5] J.K. Zhang, M.T. Cheng, D.S. Ji, Z.R. Liu, B. Hu, Y. Sun, and Y.S. Wang, Characterization of submicron particles during biomass burning and coal combustion periods in Beijing, China, Sci. Total Environ. **562**, 812–821 (2016), https://doi.org/10.1016/j.scitotenv.2016.04.015

[6] W. Knorr, F. Dentener, J.-F. Lamarque, L. Jiang, and A. Arneth, Wildfire air pollution hazard during the 21st century, Atmos. Chem. Phys. **17**, 9223–9236 (2017), https://doi.org/10.5194/acp-17-9223-2017

[7] Y. Zhang, D. Obrist, B. Zielinska, and A. Gertler, Particulate emissions from different types of biomass burning, Atmos. Environ. **72**, 27–35 (2013), https://doi.org/https://doi.org/10.1016/j.atmosenv.2013.02.026

[8] R.J. Yokelson, J.D. Crounse, P.F. DeCarlo, T. Karl, S. Urbanski, E. Atlas, T. Campos, Y. Shinozuka, V. Kapustin, A.D. Clarke, et al., Emissions from biomass burning in the Yucatan, Atmos. Chem. Phys. **9**(15), 5785–5812 (2009), https://doi.org/10.5194/acp-9-5785-2009

[9] A. Piazzalunga, C. Belis, V. Bernardoni, O. Cazzuli, P. Fermo, G. Valli, and R. Vecchi, Estimates of wood burning contribution to PM by the macro-tracer method using tailored emission factors, Atmos. Environ. **45**(37), 6642–6649 (2011), https://doi.org/https://doi.org/10.1016/j.atmosenv.2011.09.008

[10] C. Perrino, L. Tofful, S.D. Torre, T. Sargolini, and S. Canepari, Biomass burning contribution to PM10 concentration in Rome (Italy): Seasonal, daily and two-hourly variations, Chemosphere **222**, 839–848 (2019), https://doi.org/10.1016/j.chemosphere.2019.02.019

[11] Q. Zhang, J.L. Jimenez, M.R. Canagaratna, I.M. Ulbrich, N.L. Ng, D.R. Worsnop, and Y. Sun, Understanding atmospheric organic aerosols via factor analysis of aerosol mass spectrometry: a review, Anal. Bioanal. Chem. **401**(10), 3045–3067 (2011), https://doi.org/10.1007/s00216-011-5355-y

[12] N.L. Ng, M.R. Canagaratna, Q. Zhang, J.L. Jimenez, J. Tian, I.M. Ulbrich, J.H. Kroll, K.S. Docherty, P.S. Chhabra, R. Bahreini, et al., Organic aerosol components observed in Northern Hemispheric datasets from Aerosol Mass Spectrometry, Atmos. Chem. Phys. **10**(10), 4625–4641 (2010), https://doi.org/10.5194/acp-10-4625-2010

[13] J. Sandradewi, A.S.H. Prévôt, E. Weingartner, R. Schmidhauser, M. Gysel, and U. Baltensperger, A study of wood burning and traffic aerosols in an Alpine valley using a multi-wavelength Aethalometer, Atmos. Environ. **42**(1), 101–112 (2008), https://doi.org/10.1016/j.atmosenv.2007.09.034

[14] E. Liakakou, I. Stavroulas, D.G. Kaskaoutis, G. Grivas, D. Paraskevopoulou, U.C. Dumka, M. Tsagkaraki, A. Bougiatioti, K. Oikonomou, J. Sciare, E. Gerasopoulos, and N. Mihalopoulos, Long-term variability, source apportionment and spectral properties of black carbon at an urban background site in Athens, Greece, Atmos. Environ. **222**, 117137 (2020), https://doi.org/10.1016/j.atmosenv.2019.117137

[15] V. Ulevicius, S. Byčenkienė, V. Remeikis, A. Garbaras, S. Kecorius, J. Andriejauskienė, D. Jasinevičienė, and G. Mocnik, Characterization of pollution events in the East Baltic region affected by regional biomass fire emissions, Atmos. Res. **98**(2), 190–200 (2010), https://doi.org/10.1016/j.atmosres.2010.03.021

[16] S. Byčenkienė, V. Ulevicius, V. Dudoitis, and J. Pauraitė, Identification and characterization of black carbon aerosol sources in the East Baltic Region, Adv. Meteorol. **2013**, 380614 (2013), https://doi.org/10.1155/2013/380614

[17] V. Ulevicius, S. Byčenkienė, C. Bozzetti, A. Vlachou, K. Plauškaitė, G. Mordas, V. Dudoitis, G. Abbaszade, V. Remeikis, A. Garbaras, et al., Fossil and non-fossil source contributions to atmospheric carbonaceous aerosols during extreme spring grassland fires in Eastern Europe, Atmos. Chem. Phys. **16**(9), 5513–5529 (2016), https://doi.org/10.5194/acp-16-5513-2016

[18] S. Byčenkienė, V. Ulevicius, and S. Kecorius, Characteristics of black carbon aerosol mass concentration over the East Baltic region from two-year measurements, J. Environ. Monit. **13**(4), 1027–1038 (2011), https://doi.org/10.1039/C0EM00480D

[19] W.M. Kirk, M. Fuchs, Y. Huangfu, N. Lima, P. O'Keeffe, B. Lin, T. Jobson, S. Pressley, V. Walden, D. Cook, and B.K. Lamb, Indoor air quality and wildfire smoke impacts in the Pacific Northwest, Sci. Technol. Build. Environ. **24**(2), 149–159 (2018), https://doi.org/10.1080/23744731.2017.1393256

[20] S. Brasche and W. Bischof, Daily time spent indoors in German homes – Baseline data for the assessment of indoor exposure of German occupants, Int. J. Hyg. Environ. Health **208**(4), 247–253 (2005), https://doi.org/10.1016/j.ijheh.2005.03.003

[21] B.F. Yu, Z.B. Hu, M. Liu, H.L. Yang, Q.X. Kong, and Y.H. Liu, Review of research on air-conditioning systems and indoor air quality control for human health, Int. J. Refrig. **32**(1), 3–20 (2009), https://doi.org/10.1016/j.ijrefrig.2008.05.004

[22] J.L. Adgate, G. Ramachandran, G.C. Pratt, L.A. Waller, and K. Sexton, Spatial and temporal variability in outdoor, indoor, and personal $PM_{2.5}$ exposure, Atmos. Environ. **36**(20), 3255–3265 (2002), https://doi.org/10.1016/S1352-2310(02)00326-6

[23] L. Kliucininkas, E. Krugly, I. Stasiulaitiene, I. Radziuniene, T. Prasauskas, A. Jonusas, V. Kauneliene, and D. Martuzevicius, Indoor–outdoor levels of size segregated particulate matter and mono/polycyclic aromatic hydrocarbons among urban areas using solid fuels for heating, Atmos. Environ. **97**, 83–93 (2014), https://doi.org/10.1016/j.atmosenv.2014.08.010

[24] J. Zhang and K.R. Smith, Indoor air pollution: a global health concern, Br. Med. Bull. **68**(1), 209–225 (2003), https://doi.org/10.1093/bmb/ldg029

[25] A. Spinazzè, D. Campagnolo, A. Cattaneo, P. Urso, I.A. Sakellaris, D.E. Saraga, C. Mandin, N. Canha, R. Mabilia, E. Perreca, et al., Indoor gaseous air pollutants determinants in office buildings – The OFFICAIR project, Indoor Air **30(**1), 76–87 (2020), https://doi.org/10.1111/ina.12609

[26] L. Du, V. Leivo, T. Prasauskas, M. Täubel, D. Martuzevicius, and U. Haverinen-Shaughnessy, Effects of energy retrofits on Indoor Air Quality in multifamily buildings, Indoor Air **29**(4), 686–697 (2019), https://doi.org/10.1111/ina.12555

[27] I. Stasiulaitiene, E. Krugly, T. Prasauskas, D. Ciuzas, L. Kliucininkas, V. Kauneliene, and D. Martuzevicius, Infiltration of outdoor combustion-generated pollutants to indoors due to various ventilation regimes: A case of a single-family energy efficient building, Build. Environ. **157**, 235–241 (2019), https://doi.org/10.1016/j.buildenv.2019.04.053

[28] B. Kozielska, A. Mainka, M. Żak, D. Kaleta, and W. Mucha, Indoor air quality in residential buildings in Upper Silesia, Poland, Build. Environ. **177**, 106914 (2020), https://doi.org/10.1016/j.buildenv.2020.106914

[29] A. Garbaras, J. Šapolaitė, I. Garbarienė, Ž. Ežerinskis, A. Mašalaitė-Nalivaikė, R. Skipitytė, and A. Plukis, Aerosol source (biomass, traffic and coal emission) apportionment in Lithuania using stable carbon and radiocarbon analysis, Isotopes Environ. Health Stud. **54**(5), 1–12 (2018), https://doi.org/10.1080/10256016.2018.1509074

[30] M. Collaud Coen, E. Weingartner, A. Apituley, D. Ceburnis, R. Fierz-Schmidhauser, H. Flentje, J.S. Henzing, S.G. Jennings, M. Moerman, A. Petzold, O. Schmid, and U. Baltensperger, Minimizing light absorption measurement artifacts of the Aethalometer: evaluation of five correction algorithms, Atmos. Meas. Tech. **3**(2), 457–474 (2010), https://doi.org/10.5194/amt-3-457-2010

[31] E. Weingartner, H. Saathoff, M. Schnaiter, N. Streit, B. Bitnar, and U. Baltensperger, Absorption of

light by soot particles: determination of the absorption coefficient by means of aethalometers, J. Aerosol Sci. **34**(10), 1445–1463 (2003), https://doi.org/10.1016/S0021-8502(03)00359-8

[32] J. Sandradewi, A.S.H. Prévôt, S. Szidat, N. Perron, M.R. Alfarra, V.A. Lanz, E. Weingartner, and U. Baltensperger, Using aerosol light absorption measurements for the quantitative determination of wood burning and traffic emission contributions to particulate matter, Environ. Sci. Technol. **42**(9), 3316–3323 (2008), https://doi.org/10.1021/es702253m

[33] P. Zotter, H. Herich, M. Gysel, I. El-Haddad, Y. Zhang, G. Močnik, C. Hüglin, U. Baltensperger, S. Szidat, and A.S.H. Prévôt, Evaluation of the absorption Ångström exponents for traffic and wood burning in the Aethalometer-based source apportionment using radiocarbon measurements of ambient aerosol, Atmos. Chem. Phys. **17**(6), 4229–4249 (2017), https://doi.org/10.5194/acp-17-4229-2017

[34] O. Favez, I. El Haddad, C. Piot, A. Boréave, E. Abidi, N. Marchand, J.L. Jaffrezo, J.L. Besombes, M.B. Personnaz, J. Sciare, H. Wortham, C. George, and B. D'Anna, Inter-comparison of source apportionment models for the estimation of wood burning aerosols during wintertime in an Alpine city (Grenoble, France), Atmos. Chem. Phys. **10**(12), 5295–5314 (2010), https://doi.org/10.5194/acp-10-5295-2010

[35] R.M. Harrison, D.C.S. Beddows, A.M. Jones, A. Calvo, C. Alves, and C. Pio, An evaluation of some issues regarding the use of aethalometers to measure woodsmoke concentrations, Atmos. Environ. **80**, 540–548 (2013), https://doi.org/10.1016/j.atmosenv.2013.08.026

[36] P. Paatero, A weighted non-negative least squares algorithm for three-way 'PARAFAC' factor analysis, Chemometr. Intell. Lab. Syst. **38**(2), 223–242 (1997), https://doi.org/10.1016/S0169-7439(97)00031-2

[37] E. Kostenidou, B.-H. Lee, G.J. Engelhart, J.R. Pierce, and S.N. Pandis, Mass spectra deconvolution of low, medium, and high volatility biogenic secondary organic aerosol, Environ. Sci. Technol. **43**(13), 4884–4889 (2009), https://doi.org/10.1021/es803676g

[38] A.F. Stein, R.R. Draxler, G.D. Rolph, B.J.B. Stunder, M.D. Cohen, and F. Ngan, NOAA's HYSPLIT atmospheric transport and dispersion modeling system, Bull. Am. Meteorol. Soc. **96**(12), 2059–2077 (2016), https://doi.org/10.1175/BAMS-D-14-00110.1

[39] G. Rolph, A. Stein, and B. Stunder, Real-time environmental applications and display sYstem: READY, Environ. Model. Software **95**, 210–228 (2017), https://doi.org/10.1016/j.envsoft.2017.06.025

[40] C. Fountoukis and A. Nenes, ISORROPIA II: a computationally efficient thermodynamic equilibrium model for K^+–Ca^{2+}–Mg^{2+}–NH_4^+–Na^+–SO_4^{2-}–NO_3^-–Cl^-–H_2O aerosols, Atmos. Chem. Phys. **7**(17), 4639–4659 (2007), https://doi.org/10.5194/acp-7-4639-2007

[41] Y. Chen, H. Shen, and A.G. Russell, Current and future responses of aerosol pH and composition in the U.S. to declining SO_2 emissions and increasing NH_3 emissions, Environ. Sci. Technol. **53**(16), 9646–9655 (2019), https://doi.org/10.1021/acs.est.9b02005

[42] J. Ding, P. Zhao, J. Su, Q. Dong, X. Du, and Y. Zhang, Aerosol pH and its driving factors in Beijing, Atmos. Chem. Phys. **19**(12), 7939–7954 (2019), https://doi.org/10.5194/acp-19-7939-2019

[43] H. Guo, L. Xu, A. Bougiatioti, K.M. Cerully, S.L. Capps, J.R. Hite Jr, A.G. Carlton, S.H. Lee, M.H. Bergin, N.L. Ng, A. Nenes, and R.J. Weber, Fine-particle water and pH in the southeastern United States, Atmos. Chem. Phys. **15**(9), 5211–5228 (2015), https://doi.org/10.5194/acp-15-5211-2015

[44] A. Bougiatioti, I. Stavroulas, E. Kostenidou, P. Zarmpas, C. Theodosi, G. Kouvarakis, F. Canonaco, A.S.H. Prévôt, A. Nenes, S.N. Pandis, and N. Mihalopoulos, Processing of biomass-burning aerosol in the eastern Mediterranean during summertime, Atmos. Chem. Phys. **14**(9), 4793–4807 (2014), https://doi.org/10.5194/acp-14-4793-2014

[45] H. Timonen, S. Carbone, M. Aurela, K. Saarnio, S. Saarikoski, N.L. Ng, M.R. Canagaratna,

M. Kulmala, V.-M. Kerminen, D.R. Worsnop, and R. Hillamo, Characteristics, sources and water-solubility of ambient submicron organic aerosol in springtime in Helsinki, Finland, J. Aerosol Sci. **56**, 61–77 (2013), https://doi.org/10.1016/j.jaerosci.2012.06.005

[46] M. Crippa, F. Canonaco, V.A. Lanz, M. Äijälä, J.D. Allan, S. Carbone, G. Capes, D. Ceburnis, M. Dall'Osto, D.A. Day, et al., Organic aerosol components derived from 25 AMS data sets across Europe using a consistent ME-2 based source apportionment approach, Atmos. Chem. Phys. **14**(12), 6159–6176 (2014), https://doi.org/10.5194/acp-14-6159-2014

[47] C.J. Hennigan, A.P. Sullivan, J.L. Collett Jr, and A.L. Robinson, Levoglucosan stability in biomass burning particles exposed to hydroxyl radicals, Geophys. Res. Lett. **37**(9) (2010), https://doi.org/10.1029/2010GL043088

[48] S. Zhou, S. Collier, D.A. Jaffe, N.L. Briggs, J. Hee, A.J. Sedlacek III, L. Kleinman, T.B. Onasch, and Q. Zhang, Regional influence of wildfires on aerosol chemistry in the western US and insights into atmospheric ageing of biomass burning organic aerosol, Atmos. Chem. Phys. **17**(3), 2477–2493 (2017), https://doi.org/10.5194/acp-17-2477-2017

[49] J. Pauraite, K. Plauškaitė, V. Dudoitis, and V. Ulevicius, Relationship between the optical properties and chemical composition of urban aerosol particles in Lithuania, Adv. Meteorol. **2018**, 1–10 (2018), https://doi.org/10.1155/2018/8674173

[50] J.P.S. Wong, M. Tsagkaraki, I. Tsiodra, N. Mihalopoulos, K. Violaki, M. Kanakidou, J. Sciare, A. Nenes, and R.J. Weber, Atmospheric evolution of molecular-weight-separated brown carbon from biomass burning, Atmos. Chem. Phys. **19**(11), 7319–7334 (2019), https://doi.org/10.5194/acp-19-7319-2019

PAVASARĮ DEGINAMOS ŽOLĖS POVEIKIS PATALPŲ ORO KOKYBEI

J. Pauraitė [a], I. Garbarienė [a], A. Minderytė [a], V. Dudoitis [a], G. Mainelis [b], L. Davulienė [a], I. Uogintė [a], K. Plauškaitė [a], S. Byčenkienė [a]

[a] *Fizinių ir technologijos mokslų centras, Vilnius, Lietuva*

[b] *Rutgerso Naujojo Džersio valstijos universitetas, Naujasis Džersis, JAV*

Santrauka

Pavasarį deginama žolė tampa oro taršos šaltiniu, tačiau deginimo įtaka pastatų oro kokybei nėra iki galo ištirta. 1 μm skersmens kietųjų dalelių (KD_1) masės koncentracija buvo matuojama biuro Vilniuje patalpoje ir pastato išorėje (lauke) atitinkamai balandžio 25–26 ir 26–29 dienomis. Šiomis dienomis dėl žolės deginimo buvo kilę gaisrai kaimyninėse šalyse (Baltarusijoje, Ukrainoje ir Rusijoje), taip pat Vilniaus miesto prieigose esančiose vietovėse. Su gaisrais siejami išmetimai į aplinką buvo tiriami naudojant atgalinių oro masių trajektorijų (HYSPLIT) ir gaisrų žemėlapio (MODIS) metodus. KD_1 cheminė sudėtis buvo išmatuota aerozolio cheminės sudėties monitoriumi (ACSM) ir aetalometru. Organinės aerozolio dalelės fiksuotos tiek biure, tiek ir lauke (>70 % viso KD_1). Biure oro filtravimo sistema sulaikė iki 55 % KD_1 frakcijos masės koncentracijos. Nors KD_1 masės koncentracijos biure buvo mažesnės, tačiau nustatytos žemesnio pH aerozolio dalelės galėjo turėti neigiamą poveikį žmogaus sveikatai. Anglies turinčių aerozolio dalelių šaltinių analizė parodė, kad vidutiniškai 56 % šių dalelių masės koncentracijos biure galimai susidarė dėl deginamos žolės.